total effective utilization energy (Q_{all}) is the sum of Q_c and $Q_{h,dom}$, and the expression is

$$Q_{all} = Q_c + Q_{h,dom}. \quad (2)$$

The volume flow rate of water (G_w) is usually measured in the experiment. The conversion relationship between G_w and mass flow rate (M_w) can be expressed as

$$M_w = \frac{\rho_w \cdot G_w}{3600}, \quad (3)$$

where G_w is the volume flow rate of cooling water and ρ_w is the density of cooling water.

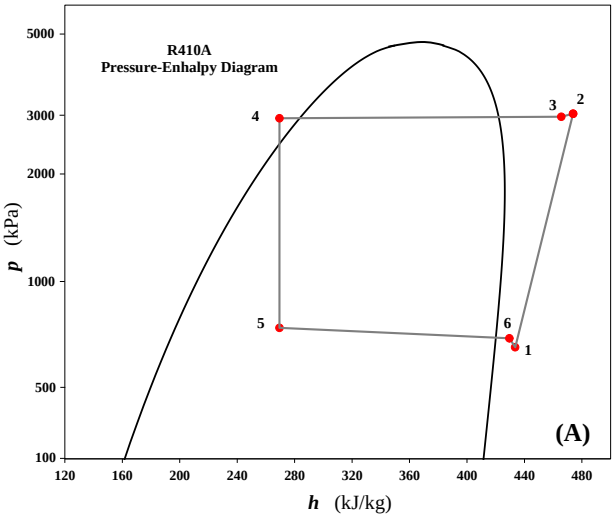

Fig. 2 The pressure-enthalpy diagram for GHP refrigerant circulation

The heat exchange between the refrigerant and cooling water at the evaporator is defined as the calculated cooling capacity ($Q_{c,cal}$). The $Q_{c,cal}$ is calculated, based on the pressure-enthalpy diagram (lg *p*-*h*) shown in Fig. 2, using the following expression:

$$Q_{c,cal} = M_{ref} \cdot (h_6 - h_5) = M_{ref} \cdot (h_6 - h_4), \quad (4)$$

where $Q_{c,cal}$ is the calculated cooling capacity; M_{ref} is the mass flow rate of the refrigerant circulating through the evaporator; h_5 and h_6 are the specific enthalpies of refrigerant at the inlet and outlet of the evaporator; h_4 is the specific enthalpy of refrigerant at the inlet of the evaporator before throttling.

The cooling capacity deviation rate (R_{devi}) is defined as the deviation between $Q_{c,cal}$ and Q_c. The calculation formula of R_{devi} is

$$R_{devi} = \frac{Q_{c,cal} - Q_c}{Q_c} \times 100\% \cdot \quad (5)$$

The mechanical power of the GHP system comes from the gas engine, and the primary energy consumption of the gas engine is expressed as

$$P_{gas} = V_{gas} \cdot LHV, \quad (6)$$

where P_{gas} is the primary energy consumption power of the gas engine, referred to as the gas consumption power; V_{gas} is the volume flow rate of natural gas consumed by the gas engine; *LHV* is the low calorific value of natural gas used in this experiment, and the calculated as a constant value (35540 kJ/m^3).

The entire heat of primary energy consumption of gas engine (P_{gas}) has four destinations: (a) the effective work converted from the thermal efficiency of the engine (P_{eng}); (b) the waste heat power in the engine-cylinder-liner coolant (P_{cyl}); (c) the waste heat power carried in the exhaust gas (P_{exh}); (d) the heat loss power of the engine (P_{loss}). The relation can be expressed as

$$P_{gas} = P_{eng} + P_{cyl} + P_{exh} + P_{loss}. \quad (7)$$

The effective power of the engine (P_{eng}) can be expressed as

$$P_{eng} = P_{gas} \cdot \eta_{eng} = \frac{T_{eng} \cdot N_{eng}}{9550}, \quad (8)$$

where η_{eng} is the thermal efficiency of the gas engine, T_{eng} is the output torque of the gas engine, and N_{eng} is the gas engine speed. In this study, the values of T_{eng} and N_{eng} are obtained through the electronic control unit controller of the gas engine.

The engine and compressors of the GHP system were connected using a V-ribbed belt. The transmission efficiency (η_t) of multi-V belt is usually 92-97 %, and in this study, η_t is considered as a constant at 95 %. The compressor power (P_{comp}) satisfies the following relationship:

$$P_{comp} = P_{eng} \cdot \eta_t. \quad (9)$$

The power source of the GHP system is natural gas, which is the primary energy source. This study introduces primary energy ratio, abbreviated as *PER*, to characterize the energy consumption performance of the GHP system [12,13]. *PER* and PER_{all} are the primary energy ratios of Q_c and Q_{all}, respectively, and the expressions are as follows:

$$PER = \frac{Q_c}{P_{gas}}; \quad (10)$$

$$PER_{all} = \frac{Q_{all}}{P_{gas}} = \frac{Q_c + \eta_h \cdot (P_{gas} - P_{comp})}{P_{gas}}. \quad (11)$$

In equation (11), η_h is the waste-heat-recovery efficiency, which can be taken as 60 % through the analysis of η_h below.

The coefficient of performance, abbreviated as *COP*, characterizes the heat pump performance of the GHP system, and the expression is expressed as

$$COP = \frac{Q_c}{P_{comp}} \cdot \quad (12)$$

Combining equations (8), (9), (10), and (12), the correlation between *PER* and *COP* can be expressed as

$$PER = COP \cdot \eta_{eng} \cdot \eta_t . \quad (13)$$

As observed from the above equation, *PER* is affected by *COP*, η_{eng} and η_t. As η_t remained constant at 95 %, *PER* is affected by *COP* and η_{eng}.

4. RESULTS AND DISCUSSION

In order to understand the part-load performance of the GHP system for cooling application, related experiments were carried out on the GHP experimental setup. The waste-heat-recovery efficiency (η_h) at different engine speeds N_{eng} (1200-2400 r/min) was studied under the no-load operation of the gas engine. According to the test conditions of IPLV in the air-cooled chilled water (heat pump) unit specified in national standard GB/T 18430.1-2007 of China, the experimental study on part-load performance of the GHP system was carried out under the cooling load rates of 25 %, 50 %, 75 %, and 100 %, respectively, and the corresponding ambient air temperatures were 24.5 ℃, 28 ℃, 31.5 ℃, and 35 ℃, respectively. The IPLVs of the GHP system (including $IPLV_{COP}$ and $IPLV_{PER}$) were calculated by analogy with EHP, and the changes of part-load performance of the GHP system were obtained.

4.1 Analysis of waste heat recovery efficiency

When the gas engine runs without load, it does not output the mechanical power, and all of the input primary energy in the system will be transferred to the engine waste heat. The GHP system in this study has been equipped with a waste-heat-recovery system for the utilization of engine-waste heat, which can transfer most of the engine-waste heat to the coolant. Part of the waste heat is recovered to domestic hot water by heat exchange through the waste-heat-recovery heat exchanger in Fig. 1. And the ratio of $Q_{h,dom}$ to P_{gas}, namely *PER*, is actually the η_h of the GHP system.

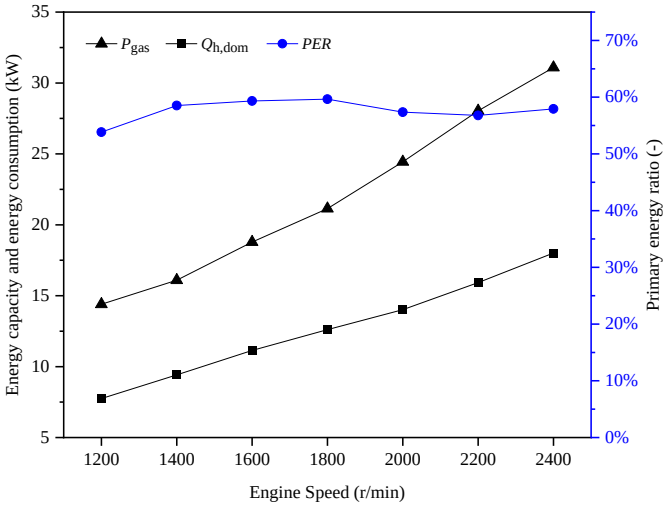

Fig.3 Variations in P_{gas}, $Q_{h,dom}$, and *PER* with engine speed when the engine runs without load.

Fig. 3 shows the influence of different N_{eng} (1200-2400 r/min) on P_{gas}, $Q_{h,dom}$, and *PER* when the ambient air temperature of the GHP system is 15 ℃ and the gas engine is under no-load operation. As shown in Fig. 3, with the increase in N_{eng}, P_{gas} and $Q_{h,dom}$ show an increasing trend. As N_{eng} increases, the gas engine needs to overcome larger internal friction work to operate, which will consume more natural gas. As more natural gas needs to be consumed, P_{gas} gradually increases. As observed from Fig. 3, *PER* is between 53.8 % and 59.6 % under different N_{eng}. This indicates that the variation of η_h is small. The increase of P_{gas} leads to more engine waste heat recovered in the system. After waste heat recovery, $Q_{h,dom}$ increases with the increase in N_{eng}. Therefore, the η_h of the GHP system in this study is approximately 60 %. When the gas engine runs under high load, more waste heat will be recovered to the domestic hot water in the GHP system.

4.2 Performance of different cooling load rate

In the national standard GB/T 18430.1-2007 of China, the performance of air-cooled chilled water (heat pump) units under different cooling load rates (L_{perc}) was explained. The IPLV which calculated by four cooling load rates can be used to evaluate the cooling performance of the GHP system more comprehensively. The main performance parameters of the GHP system at the L_{perc} of 25 %, 50 %, 75 %, and 100 % are shown in Figs. 4-6, and the corresponding ambient air temperatures are 24.5 ℃, 28 ℃, 31.5 ℃, and 35 ℃, respectively. The outlet temperature of cooling water in the system is maintained at 7 ℃. Due to the slight deviation of L_{perc} in the experimental test, the measured L_{perc} here are 27.3 %, 52.2 %, 75.2 %, and 100 %, respectively.

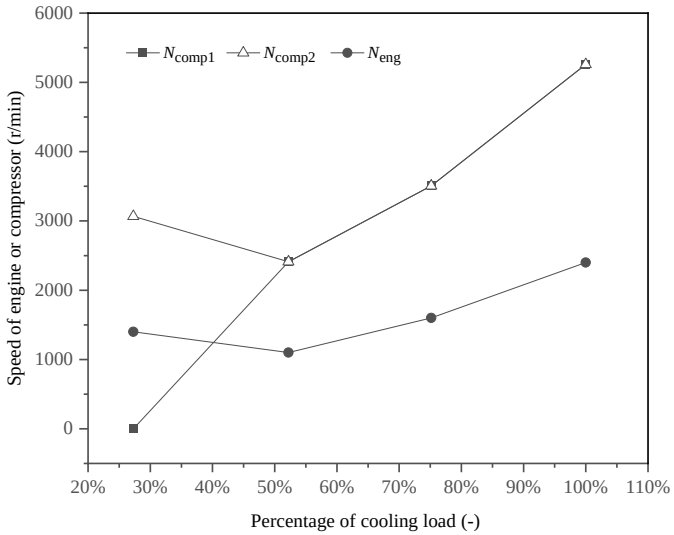

Fig.4 Variations in engine speed and compressor speed with cooling load rate.

As shown in Fig. 4, as L_{perc} increases from 27.3 % to 100 %, the speed of compressor 1 (N_{comp1}) in the GHP system gradually increases, whereas N_{eng} and the speed of compressor 2 (N_{comp2}) initially show a decreasing trend, and subsequently, show an increasing trend. When L_{perc} changes from 27.3 % to 52.2 %, the system switches from using compressor 2 only to using compressor 1 and compressor 2 simultaneously, and N_{eng} is decreased from 1400 r/min to 1100 r/min. The N_{eng} decreases, but two compressors simultaneously used will increase the refrigerant mass flow rate of the GHP system. This prompts the GHP system has a larger cooling capacity. With the further increase of L_{perc}, the heat-pump system needs a larger refrigerant circulation flow, and N_{comp} needs to increase synchronously. Therefore, N_{comp1} and N_{comp2} increase gradually. The changes of the rotational speeds of N_{comp1} and N_{comp2} are caused by the change of N_{eng}, thus N_{eng} increases gradually as well.

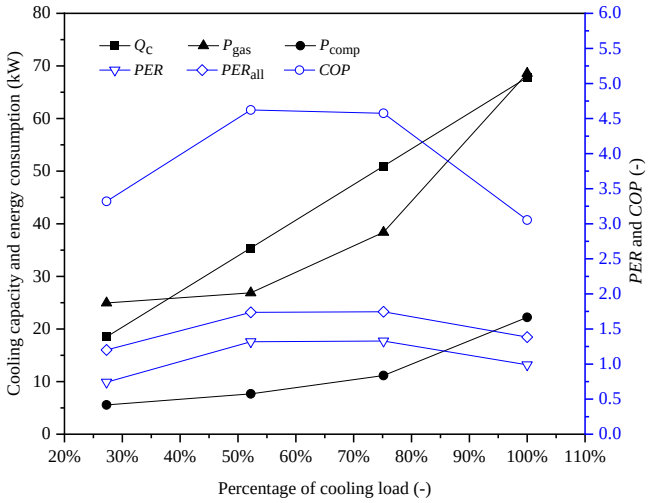

Fig.5 Variations in cooling capacity, energy consumption, *PER*, and *COP* with cooling load rate.

As observed from Fig. 5, Q_c, P_{gas}, and P_{comp} all increase with the increase in L_{perc}, whereas *PER*, PER_{all}, and *COP* initially exhibit an increasing trend, and subsequently, exhibit a decreasing trend. With the increase of L_{perc}, the compressors have larger refrigerant circulation flow rate and mechanical work, and the Q_c and P_{comp} increase accordingly. As L_{perc} increases from 27.3 % to 52.2 %, the engine speed decreases, but the energy consumption of the compressors increase. The gas engine outputs more mechanical work by increasing the torque at a lower speed, which leads to the increase in P_{gas}. In Fig. 5, as L_{perc} increase from 27.3 % to 100 %, Q_c, P_{gas}, and P_{comp} increase from 18.50 kW to 67.80 kW, 24.95 kW to 68.60 kW, and 5.57 kW to 22.20 kW, respectively. The corresponding increase times of Q_c, P_{gas}, and P_{comp} are 2.67, 1.75, and 2.99, respectively, and the increase is very significant. With the gradual increase of L_{perc}, all of *PER*, PER_{all}, and *COP* show a trend of increasing first and then decreasing, indicating that the GHP system has higher energy efficiency when it is in the middle part-load during cooling operation. *PER* and PER_{all} reach the maximum values of 1.328 and 1.745 respectively when L_{perc} is 75.2 %, and the *COP* reaches the maximum value of 4.622 when L_{perc} is 52.2 %. The reason why the maximum values of *PER*, PER_{all}, and *COP* are obtained at different L_{perc} is that the engine has a larger η_{eng} at the L_{perc} of 75.2 %, which can be drawn from Fig. 6.

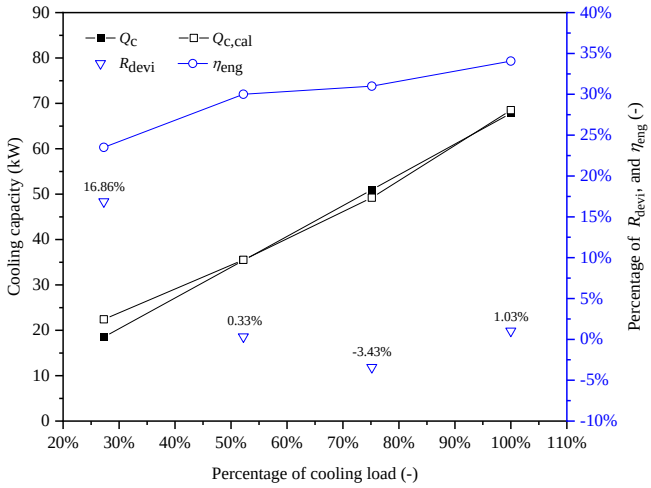

Fig.6 Variations in cooling capacity and η_{eng} with cooling load rate.

In Fig. 6, Q_c and $Q_{c,cal}$ have a similar increasing trend. Except for the L_{perc} of 27.3 %, the maximum absolute value of R_{devi} is only 3.43 % under different L_{perc}. It can be seen that the $Q_{c,cal}$ calculated based on the lg*p*-*h* diagram and expression (4) has high accuracy at medium and high cooling loads. In Fig. 6, with the increase in L_{perc}, η_{eng} increases from 23.51 % to 34.07 %. The deviation value of η_{eng} reaches 10.56 %, and the deviation is significant. When L_{perc} is 52.2 %, η_{eng} reaches 30.01 %. It is beneficial for the engine in the GHP system to output a larger proportion of mechanical work at medium and high loads. Therefore, the engine of the GHP system is more economical to operate at medium and high loads.

Based on the calculation formula of IPLV in GB/T 18430.1-2007, IPLV is the sum of the weighted values of different proportional coefficients under four cooling load rates of 25 %, 50 %, 75 %, and 100 %, and the weighted proportional coefficients are 10.1 %, 46.1 %, 41.5 %, and 2.3 %, respectively. Substituting the values of *COP* and *PER* under different L_{perc} into the calculation formula of IPLV, the values of $IPLV_{COP}$ and $IPLV_{PER}$ of the GHP system in this study are 4.435 and 1.256, respectively. It can be

seen that the integrated part-load performance of the GHP system is efficient.

5. CONCLUSIONS

In this study, the part-load performance of a novel GHP system for cooling application was investigated. The waste-heat-recovery efficiency under different N_{eng} (1200-2400 r/min) was studied under the no-load operation of the gas engine. The experimental study on part-load performance of the GHP system was carried out under the cooling load rates of 25 %, 50 %, 75 %, and 100 %. Based on the reported results, the following conclusions can be drawn.

(1) Under different N_{eng}, the values of *PER* are between 53.8 % and 59.6 %, indicating that the η_h of the GHP system is approximately 60 %. It shows that the system has an excellent waste-heat-recovery efficiency.

(2) As L_{perc} increases, Q_c, P_{gas}, and P_{comp} all increase, whereas *PER*, PER_{all}, and *COP* initially exhibit an increasing trend, and subsequently, exhibit a decreasing trend. This implies that the GHP system has higher energy efficiency when it is in cooling operation with middle part-load.

(3) When L_{perc} increases, η_{eng} increases from 23.51 % to 34.07 %. It is beneficial for the engine to output a larger proportion of mechanical work at medium and high loads. The GHP system is more economical to operate at medium and high loads.

(4) Substituting the values of *COP* and *PER* under different L_{perc} into the equation of IPLV, the values of $IPLV_{COP}$ and $IPLV_{PER}$ of the GHP system are 4.435 and 1.256, respectively. It shows that the GHP system has an efficient integrated part-load performance.

ACKNOWLEDGEMENT

This work was supported by the National Key Research and Development Program of China (No. 2021YFE0112500).

REFERENCE

[1] Roselli C, Marrasso E, Sasso M. Gas Engine-Driven Heat Pumps for Small-Scale Applications: State-of-the-Art and Future Perspectives[J]. Energies, 2021, 14(16): 4845.

[2] YANG Z, CHENG H, WU X, et al. Research on improving energy efficiency and the annual distributing structure in electricity and gas consumption by extending use of GEHP[J]. Energy policy, 2011, 39(9): 5192-5202.

[3] Tian Z, Liu F, Tian C, et al. Experimental investigation on cooling performance and optimal superheat of water source gas engine-driven heat pump system[J]. Applied Thermal Engineering, 2020, 178: 115494.

[4] Elgendy E, Schmidt J. Experimental study of gas engine driven air to water heat pump in cooling mode[J]. Energy, 2010, 35(6): 2461-2467.

[5] Elgendy E, Schmidt J. Optimum utilization of recovered heat of a gas engine heat pump used for water heating at low air temperature[J]. Energy and buildings, 2014, 80: 375-383.

[6] Liu F G, Tian Z Y, Dong F J, et al. Experimental study on the performance of a gas engine heat pump for heating and domestic hot water[J]. Energy and Buildings, 2017, 152: 273-278.

[7] Liu F G, Tian Z Y, Dong F J, et al. Experimental investigation of a gas engine-driven heat pump system for cooling and heating operation[J]. International Journal of Refrigeration, 2018, 86: 196-202.

[8] Liu F, Dong F, Li Y, et al. Study on the heating performance and optimal intermediate temperature of a series gas engine compression-absorption heat pump system[J]. Applied Thermal Engineering, 2018, 135: 34-40.

[9] Zhang Q, Yang Z, Li N, et al. A novel solar photovoltaic/thermal assisted gas engine driven energy storage heat pump system (SESGEHPs) and its performance analysis[J]. Energy Conversion and Management, 2019, 184: 301-314.

[10] Hu B, Li C, Yin X, et al. Thermal modeling and experimental research of a gas engine-driven heat pump in variable condition[J]. Applied Thermal Engineering, 2017, 123: 1504-1513.

[11] Lee W N, Kim H J, Park J B, et al. Economic analysis of heating and cooling systems from the various perspectives: Application to EHP and GHP in Korea[J]. Renewable and Sustainable Energy Reviews, 2012, 16(6): 4116-4125.

[12] Hu Y, Lv J, Huang C, et al. Experimental investigation on heating performance of a gas engine-driven heat pump system with R410A[J]. Applied Thermal Engineering, 2022, 215: 118863.

[13] Elgendy E, Schmidt J, Khalil A, et al. Performance of a gas engine driven heat pump for hot water supply systems[J]. Energy, 2011, 36(5): 2883-2889